Model of the erbium ion exchange process in lithium niobate crystals

C. Sada,* N. Argiolas, M. Bazzan, and P. Mazzoldi
INFM and Physics Department, University of Padova, Via Marzolo 8, 35131 Padova, Italy
(Received 16 May 2003; published 26 April 2004)

A model based on the Nernst-Planck equations is discussed for the trivalent ion exchange process in lithium niobate crystals. Due to the material anisotropy and the different valence state of the exchanged species, a correction to the ion flux expression is considered to include the strain effects. The model is then used to describe the erbium ion exchange in both *X*- and *Z*-cut lithium niobate crystals. In this case, the dopant in-depth profiles measured by secondary ion mass spectrometry are well fitted by the theoretical profiles predicted by the model, supporting its validity. Since the model allows to predict the dopant profile into the substrate, it can be used to tailor the process parameters.

DOI: 10.1103/PhysRevB.69.144120 PACS number(s): 66.10.Cb, 73.61.Ng

I. INTRODUCTION

The exploding demand for high speed and broadband telecommunication services has led to a push for a greater lightwave transmission capacity, requiring new and more sophisticated optical components. When complex functions are integrated in a planar geometry, in fact, reduced cost is achieved with batch processing of wafers and fewer manual interconnections, which enhances reliability. In particular the potential miniaturization of optical amplifiers has inspired considerable research interest in new Er^{3+} based amplifier materials,[1,2] lithium niobate crystals being one of these due to its excellent electro-optical, acousto-optical, and nonlinear optical properties.[3] In the last decade the erbium ions have established a key role in the development of optical communication technology as the active ion in optical signal amplification for the 1.55 μm telecommunication wavelength.[4,5] The promising results reported in literature opened the way to the use of low cost and high reliable techniques for local doping of $LiNbO_3$ crystals that maintain full compatibility with the planar geometry. Among these, the ion exchange is a promising candidate.[6–9] This technique is well known since, for artistic purposes, it was used in the past (sixth century) for coloring glasses. Its scientific and technical application,[10–13] however, is dated back to 100 years ago when it was first applied in the chemical surface tempering of glasses (potassium ion exchange).[14] Since the last decade the isovalent ion exchange has been used also for local doping of single ferroelectric crystals. In particular, proton exchange demonstrated to be a valid alternative to titanium in-diffusion for waveguide fabrication.[7] These results have prompted to study the incorporation of an active element in $LiNbO_3$ crystals with the perspective of codoping it with protons and rare-earth elements and realize an active waveguide. Within the frame of this scientific research, few years ago we demonstrated for the first time the feasibility of erbium local doping of lithium niobate by ion exchange technique.[15–18] This prompted us to (i) further investigate the complex phenomena involved in a nonisovalent ion replacement by carrying a systematic analysis over all the optimized experimental parameters; (ii) develop a model able to predict the experimental dopant in-depth profiles. In literature Nernst-Planck model has been successfully applied especially to describe the isovalent ion exchange in glasses.[10,19–26] As we will show later, it does not give correct results in the case of nonisovalent ion exchange in lithium niobate crystals. Due to the material anisotropy, in fact, a correction to the ion flux expression should be considered for including the strain effects. In this paper we will describe the role of the stress gradient and why the Nernst-Planck model lacks in treating the trivalent ion exchange in lithium niobate. To underline the critical aspects, a brief review on both the ion exchange process and the Nernst-Planck model will be presented. We will finally discuss a method to predict the dopant profile in the case of trivalent ion exchange in $LiNbO_3$.

II. ION EXCHANGE PROCESS

Ion exchange (IE) is a thermodynamic process consisting in the transfer of chemical elements between two adjacent phases, driven by the gradient of the chemical potential. Usually, the transfer takes place between a liquid phase (containing the dopant element, A^{a+}) and a solid one (the substrate to dope, containing the mobile ion B^{b+}). The ion exchange depends on (i) the thermal agitation and the nonzero mobility of certain ions in the crystals at sufficiently high temperature; (ii) the electric potential difference set up across the crystal causing an ion current to flow. In practice, the ion exchange happens when the substrate is immersed in the molten salts containing the dopant ion.

At the substrate-melt interface, the ion concentrations initially drop suddenly from finite values to zero. This is clearly a nonequilibrium situation. The thermal agitation at the interface produces random collisions in which a dopant ion replaces a matrix ion and then gradually diffuses into the substrate. The substrate ion released to the molten salt can rapidly move away from the surface and is lost in what can be considered an infinite reservoir. The process accelerates at higher temperature because of the greater thermal agitation and the less rigidity of substrate. When the crystal is lifted out of the melt while being kept at high temperature, the diffusion of the dopant continues. The dopant tends to redistribute into the substrate, moving inside, but decreasing its surface concentration. The process becomes infinitely slow only when the source of heat is removed and the substrate

allowed to cool to room temperature. The rate of the ion exchange may be influenced by (i) the mass transfer of exchanged species; (ii) the removal of products from the interface between the solid and liquid phases; (iii) the kinetics of the exchange process at the surface; and finally (iv) the transport of the dopant in the substrate. In the solid solution the mass transfer is mainly due to the diffusion process. In the liquid phase the mass transfer is driven by the diffusion and convection processes, the first being the most relevant in the interface nearby region. Convection can be enhanced by stirring the melt. However, even in the forced convection case, a region may exist near the solid-melt interface where no convective mixing occurs because of fluid friction. In order to maintain the charge neutrality the migration of ion A^{a+} into the solid phase occurs together with cation B^{b+} out-diffusion into the liquid phase. Since the driving force of the ionic species exchange is the chemical potential, i.e., the concentration gradient and electric potential gradient induced by the local nonbalance of charges, the dynamics of the process is quite complex. Up to our knowledge, the Nernst-Planck model has been successfully applied to describe the isovalent ion exchange in glass ($a=b=1$) (see, for example, Refs. 10–12,27 and 28).[29] As we will show later, it gives incorrect results in the case of nonisovalent ion exchange ($a\neq b$) when applied to lithium niobate crystals. We will discuss how to modify it by introducing the stress gradient contribution. The model prediction will be further compared to the experimental data.

III. NERNST-PLANCK MODEL

In accordance to the Nernst-Planck model, the ion exchange process can be described in terms of the one-dimensional ion flux that, for the A^{a+} ions, can be expressed as follows:

$$j_A=-D_A\frac{\partial c_A}{\partial x}+c_A\frac{D_Aq_A}{K_BT}E_{loc,charge}, \tag{1}$$

where D_A is the diffusion coefficient of A^{a+}, c_A is its concentration, q_A is the ion charge, K_B is the Boltzmann constant, T is the temperature, and $E_{loc,charge}$ is the electric field induced by the local charge imbalance. A similar expression holds for the flux of the B^{b+} ions.[30] It was found that some deviation from this equation could occur during the diffusion as a result of the correlation in the ion motion.[31] Therefore it is necessary to divide the diffusion coefficient by a factor f, depending on the ion species. This factor results from the non-random motion of the diffusing ions and depends on the diffusion mechanism, i.e., the lattice or network surrounding the moving ion. In glasses, for example, f ranges in between 0.25 and 0.65.[32] Since f is not easily calculated and is strongly connected to the diffusivity of the species, we will include it into the diffusion coefficient. If no external electric field is applied to the system, the charge compensation to consider should be

$$q_Ac_A+q_Bc_B=q_Bc_{B,0}, \tag{2}$$

where $q_B=be$ and $q_A=ae$, e being the electron charge and $c_{B,0}$ represents the B concentration in the bulk material. Moreover, the total electric current must be zero:

$$aj_A+bj_B=0. \tag{3}$$

If Eq. (1) is introduced in Eq. (3) and the charge compensation condition expressed in Eq. (2) is taken into account, it is possible to express the local electric field in terms of the ion concentration, the diffusion coefficients, and the valences (a and b) as follows:

$$E_{loc,charge}=\frac{K_BTz(M-1)}{q_B[zc_A(zM-1)+c_{B,0}]}\frac{\partial c_A}{\partial x}, \tag{4}$$

where the adimensional parameters $z=a/b$ and $M=D_A/D_B$ have been introduced. To develop this electric field, small deviation to the electrical neutrality must occur in the ionic system. However, the number of ions involved in these deviations is negligible compared to the total ionic concentrations. For this reason, in the overall material Eq. (2) can be considered valid, at least in first approximation. If Eq. (4) is inserted in Eq. (1) and if the ion flux thus obtained is introduced into the continuity equation

$$\frac{\partial c_A}{\partial t}=-\frac{\partial j_A}{\partial x} \tag{5}$$

it is possible to derive a relationship between the time variation of the ion concentration and its depth in-distribution. In this case the continuity equation can be described in terms of an effective diffusion coefficient $\tilde{D}_A[c_A]$ dependent on the ion concentration:

$$\frac{\partial c_A}{\partial t}=\frac{\partial}{\partial x}\left(\tilde{D}_A[c_A]\frac{\partial c_A}{\partial x}\right), \tag{6}$$

$$\tilde{D}_A[c_A]=D_A\left[1-\frac{z^2(M-1)c_A}{c_{B,0}+z(zM-1)c_A}\right]. \tag{7}$$

The concentration of ion A is constrained to be $0<c_A<c_{B,0}/a$, where $c_{B,0}/a$ represents the maximum value that c $_A$ can take at the surface, $c_{A,s,max}$, due to the charge neutrality condition. Moreover, it can be assumed that

$$c_A(x=0,t\geqslant 0)=c_{A,s}, \tag{8}$$

i.e., the ion replacement at the surface takes place faster than the diffusion process.[33] Obviously, the dopant ion has zero concentration inside the crystal at the starting time, that is,

$$c_A(x>0,0)=0. \tag{9}$$

In the case of nonisovalent ion exchange process, the diffusion equation, Eq. (6) must be solved numerically. Its solutions depend on the contour conditions.[34] If $M\ll 1$, the numerical solution of Eq. (6) has a different shape according to the surface value of c_A. When $c_{A,s}\ll c_{B,0}/a$, the concentration profile is similar to an erfchian function, such as in thermal diffusion processes. In the case that $c_{A,s}\approx c_{B,0}/a$, instead, the concentration tends to a steplike profile, as

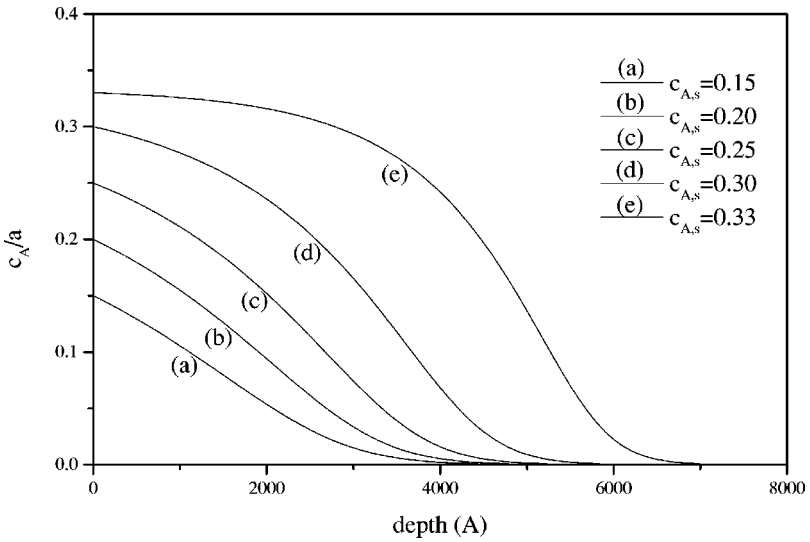

FIG. 1. Trivalent dopant concentration inside $LiNbO_3$ as predicted by Nernst-Planck model for different surface concentration values. IE parameters: $T=650\,^{\circ}\mathrm{C}$, $t=40$ h, $M=5\times10^{-5}$.

shown in Fig. 1. We focused the attention on the condition $M \ll 1$ since it is fulfilled by the erbium-lithium exchange.

The dopant incorporation is strongly influenced not only by the surface concentration $c_{A,s}$ but also by the ion diffusion coefficient and by the ion exchange conditions such as process temperature and time. In particular, Nernst-Planck model predicts that the exchanged thickness linearly increases with the square root of process duration while the role of the temperature is less significant.

Once the ion concentration profile $c_A(x)$ is determined by Eq. (6), it is also possible to evaluate the local electric-field distribution inside the substrate by means of Eq. (4). In the past it was noted[19,20,35] that the electroneutrality assumption is self-contradictory with respect to the electric field distribution. As a matter of fact no potential difference can exist if charge compensation is assumed.[21] It was thus proposed to integrate the Nernst-Planck equations taking into account that the electrostatic potential satisfies Poisson's equation and to study its time evolution. It was observed that at the beginning the high transient charge separations in liquid-liquid junctions are compensated within a period of about 10^{-7} s. As a consequence it can be concluded that deviations from electroneutrality will be important at sharp junctions for very short times. Even if we are dealing with a liquid-solid interface instead of a liquid-liquid one, we are suggested that the deviation from electroneutrality is not so problematic, especially if one considers that the number of ions involved in these deviations is negligible compared to the total ionic concentrations. An important contribution for removing this inconsistency was given by Okongwu and co-workers.[36] They pointed out that the contradiction between the electroneutrality constraint on the real charge and the nonuniform field predicted by the Nernst-Planck formalism can be removed provided that a distribution of dipoles, and therefore of dipole charges, is associated with each diffusion profile. In particular, its magnitude must be properly chosen so that solutions of the Poisson equation become exactly consistent with the diffusion generated electric field. This means that the total charge entered in the Poisson equation should contain the contribution of both the real and polarization charges. Even though the real charges vanish everywhere, the polarization charges can remain. It is an important point since the polarization charges are intimately connected with instantaneous diffusion configuration and generate the correct diffusion potential. While the real charges are arranged so that Eq. (1) is fulfilled, in general the polarization charge can vanish only when diffusion stops. A physical description of a dipole charge was not proposed by these authors who instead focused their attention toward the ion diffusion in glasses. It was Charles[32] who, in the case of glasses, gave an explanation on the origin of dipole. He presented a model that relates the diffusion process and the polarization. In crystals such as the lithium niobate this problem remains open. If the nonisovalent ion exchange occurs, a modification in the unit cell is expected. As a consequence a dipole can develop as a result of cell distortion induced by the replacement of ions with different valence state. Moreover, Okongwu and co-workers[36] demonstrated that, in the description of the interdiffusion of initially neutral samples, the residual flux j_r can exist and it can be expressed as follows:

$$\sum_{i=1,\ldots,n} Z_i j_i = -j_r \simeq 0, \tag{10}$$

where i runs over the diffusing ions. Equation (10) describes the tendency to minimize the electrostatic energy through the minimization of the net accumulation of charge. The residual flux j_r is small relative to each $|Z_i j_i|$ term and indeed it leads to diffusion profiles for which

$$\sum_{i=1,\ldots,n} Z_i c_i = 0 \tag{11}$$

as required. The zero-current condition is properly designated as the ''quasisteady'' approximation, since all the steady-state systems, immersed in neutral media must satisfy Eq. (10) with the equality sign exactly. Moreover, if Eq. (10) is considered, it can be demonstrated that c_A and c_B step discontinuities at the interface vanish if and only if the anion charge concentration per unit volume is the same on both sides. In this case the results obtained by Eqs. (1) (10) are the

same and the arguments described in the previous paragraph are coherent. It is important to underline that from a mathematical point of view, the electroneutrality requirement must be distinguished from the way in which this requirement is imposed on a system of diffusion equations. In a liquid-solid interface all the terms in Eq. (2) have discontinuities at the junction and therefore Eq. (2) is inappropriate as a restriction on a set of differential equations. For this reason, Eq. (10) guarantees a more profitable and less prone to mathematical errors which can generate contradictions.

If one compares the prediction of the Nernst-Planck model to the experimental results it results in a clear discordance especially in the dopant profile shape at the interface with the substrate. In the following section we will discuss how one can face this problem.

IV. MODIFICATION OF THE NERNST-PLANCK MODEL

In Sec. III, the strain energy induced by the diffusion process has not been taken into account. Since the dopant incorporation induces a modification in the unit-cell size due to its different ionic radius and valence state with respect to the replaced element, the ion flux can be thus affected by the crystal structure response. It is of primary importance to introduce this contribution in order to properly fit the experimental data. At our knowledge, no models have been proposed yet for describing the crystal structure response in case of the nonisovalent ion exchange. In the present work, some assumptions will be introduced and a model will be presented.

In analogy with the ''electric'' term present in the Nernst-Planck model [Eq. (1)], we can express the contribution of stress as follows:

$$\frac{D_A}{KT} F_{stress} c_A , \tag{12}$$

where F_{stress} is a force connected to the crystal structure modification. Since the crystal structure feels the effects of the different atomic coordination and dimension of the dopant ion with respect to the replaced species of the substrate, we assume that

$$F_{stress} = V \frac{\partial \sigma}{\partial x}, \tag{13}$$

where V indicates the exchanged layer volume and σ is the stress. In the following, for the sake of simplicity, we will consider V as N times the cell volume where N refers to the number of cells involved in the ion exchanged process. It is not trivial to estimate its absolute value so it will be necessary to introduce some further assumptions. According to Eq. (13) the total ion flux presents the following form:

$$j_{A,\mathrm{tot}} = -D_A \frac{\partial c_A}{\partial x} + c_A \frac{q_A D_A}{K_B T} E_{loc} + \frac{D_A}{K_B T} c_A V_A \frac{\partial \sigma}{\partial x}, \tag{14}$$

being the sum of two terms, one containing the stress contribution and the other being as reported in Eq. (1). In particular V_A indicates the value of V after ion exchange, that is, when A^{a+} has replaced B^{b+}. A similar expression holds for the ion B^{b+} where, in this case, V_B indicates the volume before ion exchange takes place (no B replacement). The determination of an accurate expression of the stress gradient plays a key role and will be discussed later.

The introduction of such a term in the ion flux expression takes into account that the local field gets contributions from (i) the different mobilities of each exchanging element and (ii) the role of the crystal deformation. If Eq. (14) is introduced in Eq. (3) and we express the boundary condition as in Eq. (2), the local electric field results as follows:

$$E_{loc} = E_{loc,charge} + E_{loc,stress}, \tag{15}$$

where $E_{loc,charge}$ is given by Eq. (4) and $E_{loc,stress}$ gathers all the stress contributions. In particular it follows that

$$E_{loc,stress} = \frac{1}{q_B} \frac{\partial \sigma}{\partial x} \frac{V_B [z c_A (1 - \eta M) - c_{0,B}]}{z c_A (zM - 1) + c_{0,B}}, \tag{16}$$

where $\eta = V_A / V_B$ has been introduced.

Once the ion exchanged species are defined (so that z is fixed) and the border conditions are applied, the numerical solution of Eq. (5) depends mainly on choice of the stress gradient profile and, consequently, on various parameters: (i) M, $c_{A,s}$, (ii) η, and (iii) the ion exchange parameters (processing time and temperature).

A. Hypothesis on stress

As previously quoted, the ion exchange process involves the modification of the substrate surface so as to remind a film formation on the surface. Stress σ can be introduced in a thin film due to differential thermal expansion between it and the substrate, due to lattice misfits or due to chemical interaction with its substrate. On a planar substrate the stress due to differential thermal expansion experienced by the film is biaxial, the stress acting along the two principal axes in the plane of the film. Since the ion exchange process involves the replacements between differently sized ions, volume differences may occur. In the case of the nonisovalent case, moreover, also the valence state of the species involved should be taken into account. If the substrate is allowed to relax to the equilibrium volume corresponding to the new ions, no residual stresses would develop. However, the ion exchange process normally is carried out at temperatures where the crystal relaxation does not occur. Hence, the volume differences have to be accommodated by elastic strains accompanied by the building up of residual stresses. It is worth mentioning that the volume of the exchanged layer differs from the equilibrium one obtained with bulk doping. Instead, the volume of the exchanged layer is forced to remain closer to the value before the process occurrence by mechanical constraints exerted by the much thicker substrate in the directions that are parallel to surface. This discrepancy is the direct cause for the evolution of the ion exchange stresses. In literature many formulations of the stress were proposed for the isovalent ion exchange in glass, based on an isotropic model and on the assumption that the stress should be planar.[37] As the components parallel to the surface are

concerned, they have the same value only in an isotropic medium. In analogy to the thermal stress, in literature it is reported that

$$\sigma(x)=\frac{(\Delta V)_d E_y C_A(x)}{1-\nu}+\frac{(\Delta V)_d E_y}{L(1-\nu)}\int_{-L}^{L} C_A(x')dx', \tag{17}$$

where

$$C_A=\frac{c_A}{c_A+c_B} \tag{18}$$

represents the concentration fraction of A, $(\Delta V)_d$ indicates the volume variation

$$(\Delta V)_d=\frac{V_A-V_B}{3V_B}=\frac{1}{3}(\Delta V)_r \tag{19}$$

before (subscript B) and after (subscript A) the ion exchange process occurs. Moreover, E_y is the Young modulus and ν is the Poisson ratio. When nonisotropic crystals are considered, however, the stress components parallel to the surface differ. This complication, unfortunately, is not solved by approximating the lithium niobate crystal as an isotropic medium. As a consequence, the isotropic assumption must be revised as the stress expressed by Eq. (17) is not appropriate. Since an *a priori* model of stress distribution inside the crystal is not trivial, some hypotheses should be made. The introduction of the stress term strongly modifies the distribution of the local electric field. The crystal limits the ion exchange process since it requests energy for the reorganization of its lattice structure. We started from the idea that the stress contribution should ''play against'' the mobility contribution. From a theoretical point of view this assumption comes from the experimental evidence that the ion exchanged depth is less than that expected from the prediction of the original Nernst-Planck model. In the last case, in fact, the dopant ions are driven into the substrate by the dopant gradient concentration as well as the local electric field $E_{loc,charge}$. We assumed that a region exists in which the piezoelectric field produced by the stress gradient partially compensates $E_{loc,charge}$ so that the total electric field experienced by the ions, E_{loc}, is weaker than that predicted by the Nernst-Planck model. By means of this assumption the local electric field caused by the stress term, $E_{loc,stress}$, gives rise to a sort of blocking process which hinders the further in-diffusion of the dopant ions. In this region the contribution to the dopant in-diffusion comes only from the concentration gradient, so that dopant incorporation still occurs but is less effective. The proper shape of the stress gradient was determined assuming that $E_{loc,stress}$ was likely to have a shape similar to $-E_{loc,charge}$ so that a dip should occur in E_{loc} in order to simulate the presence of the blocking forces. The fact that the experimental dopant profiles present a plateau near the surface, followed by a decreasing shape toward the substrate interface, suggests us that this dip should lay about the end of this plateau. The $E_{loc,stress}$, and consequently E_{loc}, therefore contains some free parameters that should be properly chosen for $j_{A,tot}$ to remain positive. As a first step, we solved Eq. (5) and find these free parameters by fitting the experimental dopant profiles. Once the best free parameters were identified, we derived the expression of the resultant $\partial\sigma/\partial x$. In analogy to Eq. (17) we split the resultant stress gradient profile into two terms, one mainly dependent on the dopant concentration gradient, the other giving the peak in correspondence of the dip in E_{loc}. The free parameters were then expressed in terms of known quantities depending on the crystal structure and dopant concentration as suggested by Eq. (17). We found that the most likely function should have the following gradient:

$$\frac{\partial\sigma}{\partial x}=\frac{\partial c_A}{\partial x}c_{0,B}K_1 \times\frac{c_A z^2 M(\eta+1)-c_A z(z+1)+c_{0,B}(1-z)}{[c_{0,B}+c_A(1-z)^2+c_A z(zM-1)+c_{0,B}]c_{0,B}} \times\frac{zc_A(zM-1)+c_{0,B}}{zc_A(z-\eta)+c_{0,B}(\eta-z)}, \tag{20}$$

where $\eta=V_A/V_B$, $M=D_A/D_B$, $z=q_A/q_B$ and finally

$$K_1=\frac{(\Delta V)_d c_{ij}}{1-\nu}. \tag{21}$$

In particular c_{ij} is the elastic stiffness and ν represents the Poisson ratio ($\nu=0.23$ for x-cut crystals, $\nu=0.43$ for Z cut), which include all the information on the crystal structure.[38,39] The expression reported in Eq. (20) guarantees the presence of a dip in the electric field and therefore the presence of a sort of blocking force. In the case of an X-cut crystal, it is worth mentioning that the stress given by Eq. (20) contains the contribution of both the two components parallel to the surface. In this way, we consider the overall effect of the stress on the surface. Furthermore, we underline that all the physical parameters have been expressed as relative values since ion process is so complex that the diffusivity of each species is strongly influenced by the other.[29,40,41] It is worth mentioning that in our model we do not consider explicitly the effect of the buildup of the space charges. As a matter of fact, they can contribute to the cell volume modification via the piezoelectric effect and to E_{loc}. In the last case they can account for the fact that it is weaker than that predicted by the Nernst-Planck model. However, since their effect is complex and they are difficult to estimate, we prefer to include their contributions in the term $(\Delta V)_d$ and in η, respectively. Once the exchanging species are known (i.e., z is fixed), the free parameters η [and consequently $(\Delta V)_r=(V_A-V_B)/V_B$], M, and c_{ij} must be introduced in order to define $\partial\sigma/\partial x$: for this reason, further assumptions must be considered.

η and c_{ij}

Concerning the elastic stiffness, its values are tabulated in literature by many authors[38] so no further discussion is needed. On the contrary, some assumptions should be introduced for estimating η since it depends on the volume before and after the ion exchange. In first approximation, V_B can be

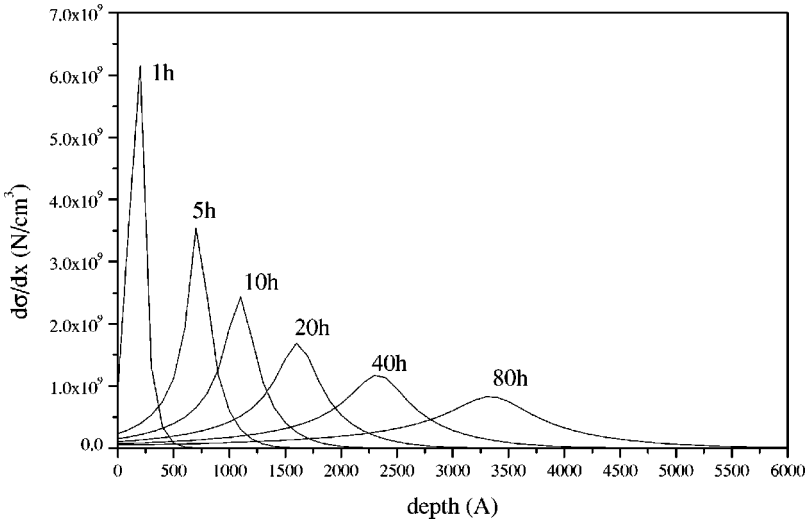

FIG. 2. Dependence of $\partial\sigma/\partial x$ on processing time. IE parameters: $T=650\,^{\circ}\mathrm{C}$, $c_{A,s}=0.33$, $M=5\times10^{-5}$, $(\Delta V)_r=0.1\%$, $z=3$.

derived by thermal-expansion consideration so that it can be generally expressed as $V_B=V_{B,RT}f(T)$ where $f(T)$ is a proper function of temperature and $V_{B,RT}$ refers to the volume value at room temperature (RT). In case of lithium niobate crystals up to the second order it results in[38,42]

$$\frac{V_B}{V_{B,RT}}=1+(2\alpha_{11}+\alpha_{33})(T-T_{RT})+(2\beta_{11}+\beta_{33})(T-T_{RT})^2. \tag{22}$$

Since lithium niobate is characterized by a hexagonal cell, its cell volume is equal to $V_{B,RT}^{cell}=(\sqrt{3}/2)a^2c=318$ Å^3 using the lattice parameters reported in Refs. 38 and 39. In the range 550–700°C the relative volume variation induced by the thermal expansion is about 0.25–0.35 %. A similar approach can be used also for V_A, so that

$$\frac{V_A}{V_{A,RT}}=f'(T), \tag{23}$$

where $f'(T)$ is a suitable function of temperature which, in principle, might not be equal to $f(T)$. In fact, in the exchanged layer a structure modification can occur so that thermal stresses can develop. However, it has been shown that[37] in general the thermal stress is less than 1% of the contribution deriving from accommodation of different-sized ions. For this reason, we assume that $f'(T)=f(T)$. If this is the case, we obtain

$$\eta=\frac{V_A}{V_B}=\frac{V_{A,RT}}{V_{B,RT}}=\frac{\sum_{i=1}^{N}V_{A,RT}^{cell,i}}{\sum_{i=1}^{N}V_{B,RT}^{cell,i}}, \tag{24}$$

where the subscript $cell$ refers to the lattice unit cell and i runs over all the N cells we divide V in. While it is clear that $V_{B,RT}=NV_{B,RT}^{cell}$, as far as $V_{A,RT}$ is concerned we can perform $\Sigma_{i=1}^{N}V_{A,RT}^{cell,i}$ over a proper number of cell N' so that

$$N'V_{A,RT}^{cell,max}\approx\sum_{i=1}^{N}V_{A,RT}^{cell,i}, \tag{25}$$

where $V_{A,RT}^{cell,max}$ represents the maximum cell volume obtained for maximum lattice parameter values found in the exchanged layer. In this way, we can simplify Eq. (24) by factorizing N':

$$\frac{V_{A,RT}}{V_{B,RT}}=\frac{N'}{N}\frac{V_{A,RT}^{cell,max}}{V_{B,RT}^{cell}}. \tag{26}$$

If we suppose that the ion exchange process preserves the hexagonal cell, $V_{A,RT}^{cell,max}$ can be expressed as follows:

$$V_{A,RT}^{cell,max}=\frac{\sqrt{3}}{2}a'^2c', \tag{27}$$

where a' and c' are the lattice parameters of the cell when A^{a+} replaces B^{b+}. Consequently,

$$(\Delta V)_r=\left[\frac{N'}{N}\left(\frac{\Delta a}{a}+1\right)^2\left(\frac{\Delta c}{c}+1\right)-1\right], \tag{28}$$

where $\Delta a=a'-a$ and $\Delta c=c'-c$, respectively. In this way $(\Delta V)_r$ has been expressed in terms of a measurable quantity by x-ray-diffraction analysis, i.e., the maximum lattice mismatch induced by the ion exchange process. In particular, a cell shrinking of about 0.1% corresponds to $\Delta a/a=\Delta c/c=0.05\%$, i.e., to a lattice mismatch with the magnitude order about 10^{-4}. Once $(\Delta V)_r$ is known, η can be easily calculated.

In the following paragraph we will discuss (i) the influence of the ion exchange conditions on the stress gradient profile and (ii) the role of each free parameter such as M and η.

B. Influence of the ion exchange parameters on stress

Figure (2) shows the stress gradient profiles for various processing times. Under our hypothesis, the stress gradient presents a peaked shape which gradually decreases and

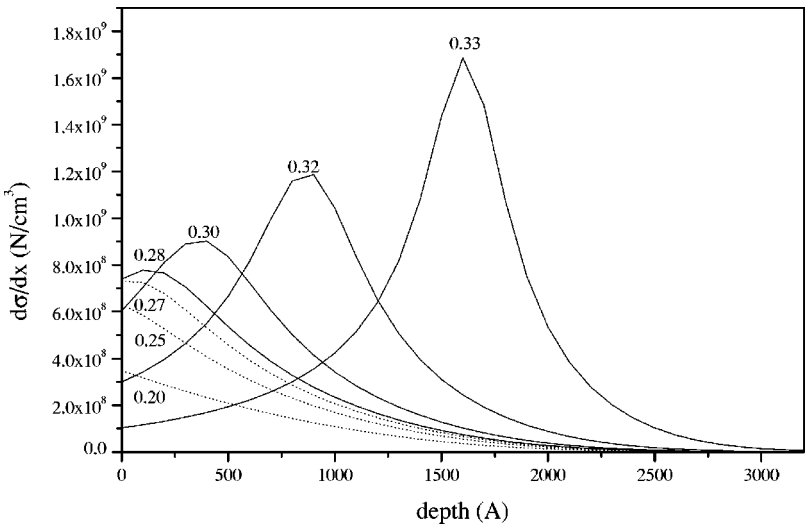

FIG. 3. Dependence of $\partial\sigma/\partial x$ on dopant surface concentration $c_{A,s}$. IE parameters: $t=20$ h, $M=5\times10^{-5}$, $(\Delta V)_r=0.1\%$, $z=3$.

broadens with increasing processing time. For short processing times the crystal structure is subjected to a higher stress since the ion redistribution, necessary for overcoming the different coordination state of the in-diffused species with respect to the out-diffused one, is not complete. Moreover, the stress gradient lowers when temperature increases due to the fact that the matrix is less rigid and the ions are more mobile.

In Fig. 3 the stress gradient is reported in function of the dopant surface concentration for ion exchange temperature equal to 650 °C and process duration equal to 20 h.

For $0\leqslant c_A\leqslant 0.27$, the stress gradient shows a monotonically decreasing shape and its surface value linearly increases with $c_{A,s}$. This behavior agrees with the fact that at lower dopant concentration, the substrate ''effort'' to accommodate the new ions is lower. For higher values of dopant surface concentration, the stress gradient profile shows a peaked shape with the maximum linearly increasing with the dopant surface concentration. In this sense $c_{A,s}=0.27$ can be considered a border value above which a different dynamics in the dopant incorporation occurs. When the dopant concentration at the surface increases above this limit, the number of dopant ions in-diffused inside the substrate are relevant and the exchanged layer reaches a significant thickness as well. Therefore, along the exchanged depth, the dopant concentration is quite high and the energy to be spent by the crystal for accommodating the dopant increases. In this case the strain relaxation is more difficult since the modified thickness is now significant. Consequently, at fixed D_A/D_B ratio, higher stress develops at the interface between the exchanged layer and the substrate itself with respect to that observed for a lower dopant concentration.

In Fig. 4 we show the dependence of the stress gradient on the D_A/D_B ratio in the case of $c_{A,s}$ equal to 0.33. As it can be seen, doubling the value of the D_A/D_B ratio, the stress gradient peak decreases. The ion redistribution is in fact facilitated by the higher ion mobility.

In the case of a low dopant surface concentration (i.e., $c_{A,s}=0.2$), a different shape can be observed [see Fig. 5]. The stress gradient shows a monotonic decrease similar to an erfchian function.

C. The dopant in-depth profile

As described in the case of Nernst-Plack model, the dopant concentration profile can be determined integrating the

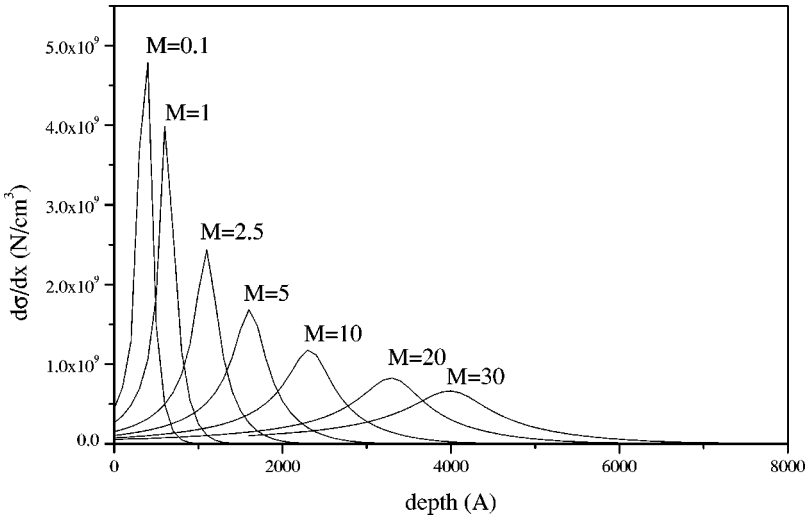

FIG. 4. Dependence of $\partial\sigma/\partial x$ on $M=D_A/D_B$ normalized to 10^{-5}. IE parameters: $t=20$ h, $T=650$ °, $c_{A,s}=0.33$, $(\Delta V)_r=0.1\%$, $z=3$.

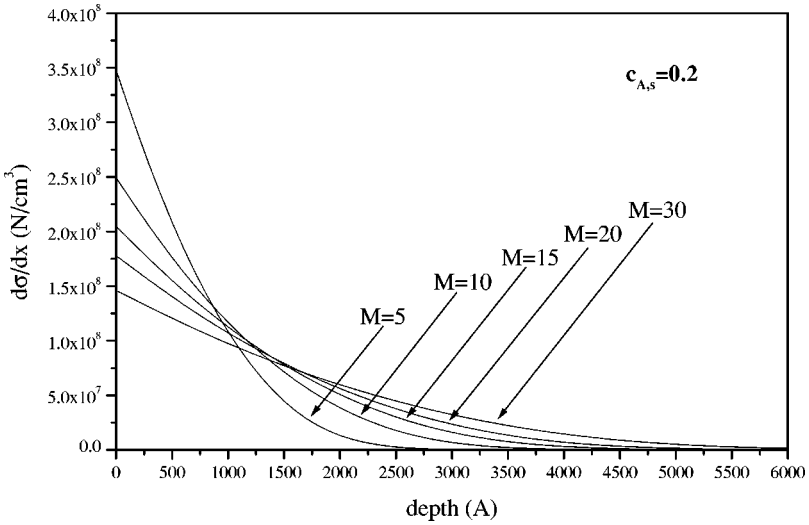

FIG. 5. Dependence of $\partial\sigma/\partial x$ on dopant surface concentration $c_{A,s}$. IE parameters: $t=20$ h, $(\Delta V)_r=0.1\%$, $z=3$. M values label the corresponding curve normalized to 10^{-5}.

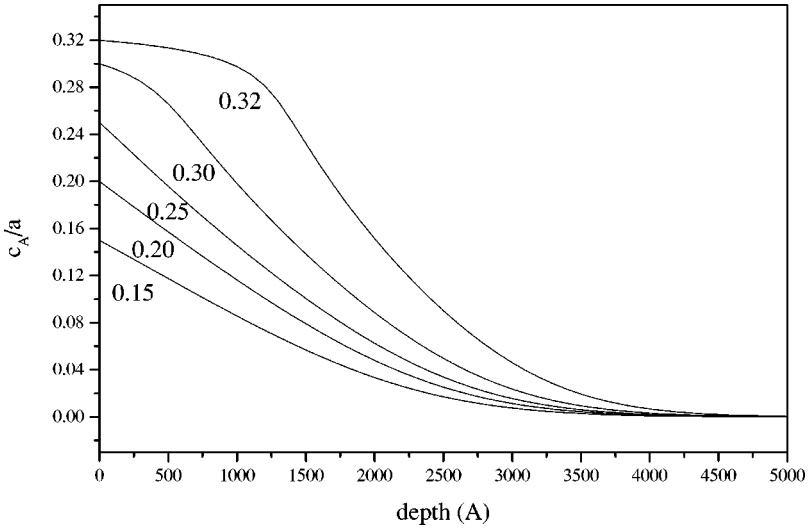

FIG. 6. Dopant incorporation for various surface concentrations. IE parameters: $T=650\,^{\circ}$C, $t=20$ h, $(\Delta V)_r=0.1\%$, $M=6.5\times10^{-5}$.

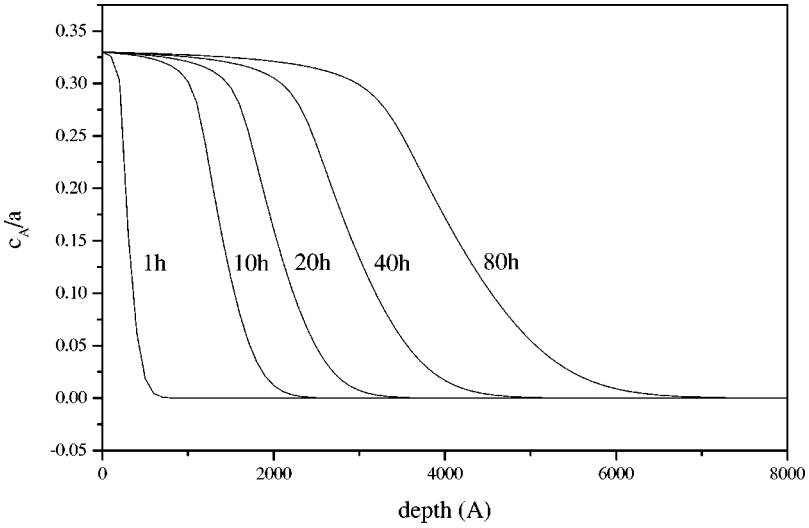

FIG. 7. Dopant incorporation for different processing time. IE parameters: $T=650\,^{\circ}$C, $c_{A,s}=0.32$, $(\Delta V)_r=0.1\%$, $M=5\times10^{-5}$.

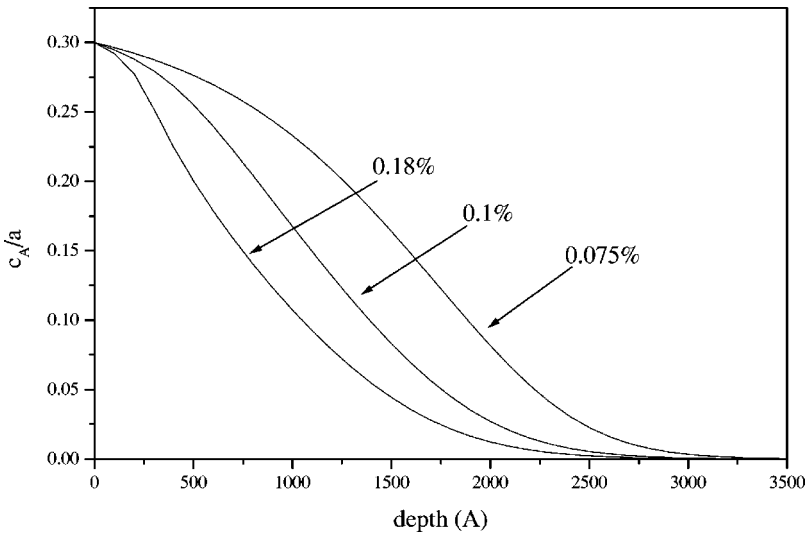

FIG. 8. Dopant in-depth profile obtained by TIE model for different $(\Delta V)_r$ values. IE parameters: $T=650\,^{\circ}\mathrm{C}$, $t=20$ h, $c_{A,s}=0.30$, $M=5\times10^{-5}$.

continuity equation, Eq. (5), taking into account the border conditions. In order to perform such integration, Eq. (20) should be introduced inside Eq. (16). Finally, the expression of the local electric field thus obtained should be inserted in Eq. (14). In Figs. 6 and in 7 we report the dependence of the dopant profile on surface dopant concentration and processing time, respectively, obtained from the integration of Eq. (5).

As it can be observed, if $c_{A,s}$ is lower than 0.27, the dopant profile resembles an erfchian function, similarly to what was obtained by the thermal diffusion process from a thin film. As the dopant surface concentration increases, the surface nearby region smoothes till a plateau is formed. The tail does not have a sharp decrease as obtained by the Nernst-Planck model. The introduction of the stress contribution, in fact, does not influence the role of temperature and processing time in the dopant incorporation. It strongly modifies, instead, the tail of the dopant in-depth profile. Under the same process conditions, it reduces the exchanged depth. A direct confirmation of this fact can be immediately evidenced in Fig. 8.

When the modification of the cell volume is higher the stress gradient and the dopant in-depth profile are limited in depth. Finally Fig. 9 directly compares the dopant profile obtained by Nernst-Planck and our model (referred with the acronym TIEM, trivalent ion exchange model) under the same preparation conditions.

It underlines that the introduction of the stress contribution smoothes the dopant in-depth profile broadening the tail at the substrate interface. The dopant incorporation depth is about 25% less than that obtained by Nernst-Planck model. This behavior is observed also for low $c_{A,s}$ values and for different process durations (not here reported).

In the paragraph dedicated to the experimental results, this model will be applied to the erbium ion exchange. The free parameters $M=D_A/D_B$, ΔV_r, and $C_{A,sup}$ will be changed in order to fit the experimental in-depth profiles obtained by secondary ion mass spectrometry. As it will be shown, the model here described correctly fits the experimental data.

V. EXPERIMENTAL RESULTS: ION EXCHANGE IN $LiNbO_3$

In this paragraph we will compare the erbium profile simulated by TIE model with the experimental one obtained

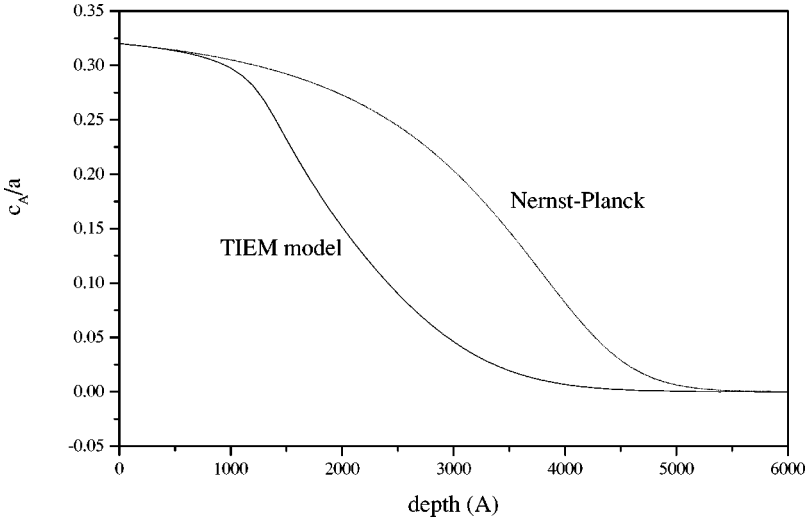

FIG. 9. Comparison between dopant profile obtained by Nernst-Planck and TIE model, respectively. IE parameters: $T=650\,^{\circ}\mathrm{C}$, $t=40$ h, $(\Delta V)_r=0.1\%$, $M=5\times10^{-5}$. Left: $c_{A,s}=0.32$. Right: $c_{A,s}=0.25$.

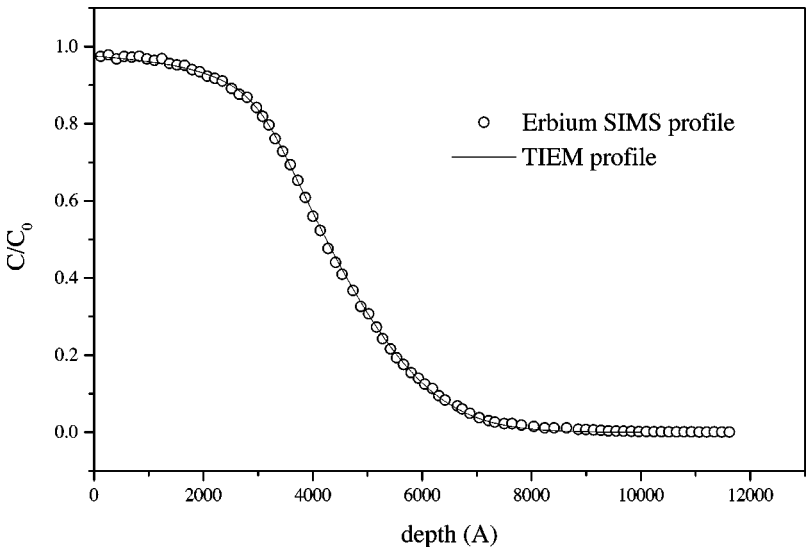

FIG. 10. Erbium SIMS profile compared with theoretical fit given by TIE model in an *X*-cut crystal. IE parameters: $Er_2(SO_4)_3 = 0.18$ wt. %, $t = 20$ h, $T = 650\,^{\circ}C$, TIEM parameters: $M = 1.8 \times 10^{-4}$, $\Delta V_r = -0.12\%$.

by secondary ion mass spectrometry (SIMS) analysis (experimental procedures and apparatus are reported elsewhere[18]). The samples were prepared by immersing the crystal slide in a mixture of lithium, sodium, potassium, and erbium sulfates molten with a slow heating rate (100 °C). The processing temperature and time were varied in the range 570–750 °C and 10–120 h respectively. The details of the sample preparation by the Ion Exchange technique are described in Refs. 17 and 18. From all the exchanged crystal analyses, in the following only few examples will be presented. As previously described, the simulation of the experimental erbium in-depth profile depends on few parameters (M, ΔV_r, and $c_{A,s}$) which should be entered after the ion exchange conditions are defined (such as temperature and time). Since these parameters are not known in literature, a first step of our work was devoted to define their best values. After their determination, the model can be used for defining the ion exchange conditions in order to tailor the erbium-doped lithium niobate crystal properties. We will also show that ΔV_r can be correlated with the lattice-parameter change induced by the process. This correlation confirms the consistency of the model and the validity of the assumptions introduced. Moreover it supports the physical meaning of the those parameters that, at first sight, can be considered mainly phenomenological parameters. TIE model therefore can give interesting pieces of information on the dynamics of the process. In fact, a simulation on the local electric field, on the ion flux, and on the stress gradient distributions can be obtained. In Fig. 10 erbium SIMS profile is compared to the prediction of the TIE model.

As it can be seen, the predictions of the model fit successfully the experimental in-depth profile independently of the preparation conditions. In Fig. 11 the TIE model is applied for a process duration of about 90 h at temperature equal to 675 °C. Even if the shape of the SIMS profile is smoother than those previously reported TIE simulation well agrees with it. From the comparison between experimental results and TIE predictions, it emerges that only negative values of ΔV_r have to be used in order to properly fit the compositional erbium profile. This means that the unit cell shrinks when erbium incorporation occurs. We can compare the $(\Delta V)_r$ values obtained experimentally with those predicted

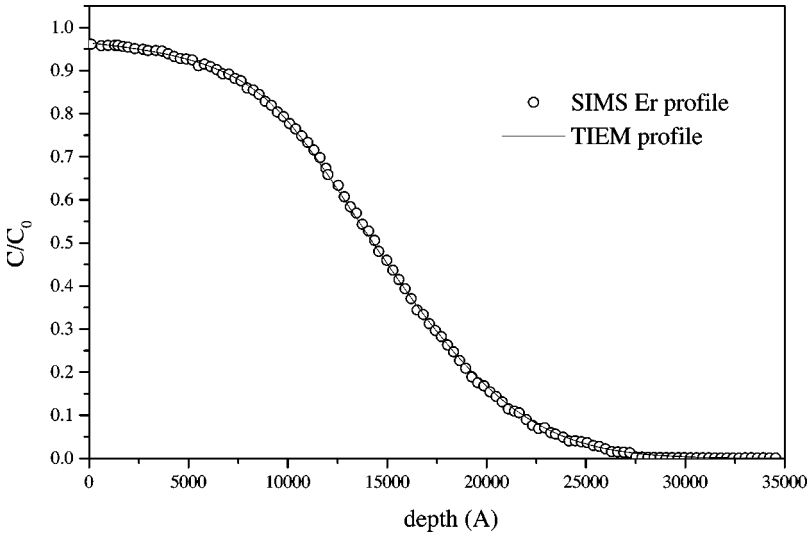

FIG. 11. Erbium SIMS profiles compared with theoretical fit given by TIE model in an *X*-cut crystals. IE parameters: $Er_2(SO_4)_3 = 0.35$ wt. %, $t = 90$ h, $T = 675\,^{\circ}C$. TIEM parameters: $M = 1.02 \times 10^{-3}$, $\Delta V_r = -0.14\%$.

TABLE I. Comparison between $(\Delta V)_r^{expt}$ and $(\Delta V)_r^{theor}$. IE conditions: $c_{Er_2(SO_4)_3}=0.18$ wt. %, $T=650\,^{\circ}$C.

Cut	Process duration (h)	$(\Delta V)_r^{expt}$ (%)	$(\Delta V)_r^{theor}$ (%)
X	40	−0.14	−0.16
X	80	−0.12	−0.13
Z	40	−0.08	−0.07
Z	80	−0.06	−0.07

by the TIE model for $N'/N\approx 1$. In Table I we report the experimental and theoretical values of $(\Delta V)_r$, the first derived by *X*-ray-diffraction (XRD) measurements (experimental procedure and apparatus for XRD analysis are described in Ref. 43), the other by best-fit simulation of the SIMS erbium profile.

As it can be seen, the difference between the experimental results and the theoretical prediction is less than 15%. A final remark on the factor N'/N is now necessary. It is interesting to notice that for N'/N about 10–15 % the difference between $(\Delta V)_r^{expt}$ and $(\Delta V)_r^{th}$ would vanish. However, since the lattice parameters are affected by experimental errors, it is not possible to quantitatively determine N'/N without assumptions. The comparison here proposed, is in any case self-consistent, since both in the theoretical and experimental approaches the maximum lattice mismatch is considered. This comparison is significant for two reasons: first as it gives a further confirmation of the consistency of TIE model from the structural point of view. Second, it also evidences that the parameters introduced in the model, necessary for the simulation of the erbium profile, have a specific physical meaning and should not be considered only phenomenological.

VI. CONCLUSIONS

In this paper we showed why the Nernst-Planck model lacks in treating the trivalent ion exchange in lithium niobate and how the stress gradient can play an important role in the process. Making the assumption that the stress gradient influences the local-field distribution inside the substrate, the dopant in-depth profile was simulated. In particular case of lithium niobate crystals, an expression for the stress gradient profile was proposed in agreement with the building-up of the blocking forces already invoked by many authors[13] to explain the process. The model predictions were tested for different preparation conditions and supported the consistency of the model assumptions. This model allows to identify the ion exchange conditions in order to tailor the erbium-doped lithium niobate crystal properties.

ACKNOWLEDGMENTS

The authors kindly acknowledge Dr. F. Segato for contributing to the code implementation of the Nernst-Planck model and Johannes T. Gambari from the Physics Department of the Imperial College London for the text revision and the fine discussions.

*Author to whom correspondence should be addressed. Email address: sada@padova.infm.it

[1] M.N. Armenise, M. De Sario, C. Canali, A. Carnera, P. Mazzoldi, and G. Celotti, J. Appl. Phys. **54**, 6223 (1983).
[2] I. Baumann, R. Brinkmann, M. Dinand, W. Sohler, L. Beckers, Ch. Buchal, M. Fleuster, H. Holzbrecher, H. Paulus, K.-H. Müller, Th. Gog, G. Materlik, O. Witte, H. Stolz, and W. von der Osten, Appl. Phys. A: Mater. Sci. Process. **64**, 33 (1997).
[3] P.J. Chandler, L. Zhang, and P.D. Townsend, Electron. Lett. **26**, 332 (1990).
[4] P. Becker, R. Brinkmann, M. Dinand, W. Sohler, and H. Suche, Appl. Phys. Lett. **61**, 1257 (1992).
[5] M. Fleuster, Ch. Buchal, E. Snoeks, and A. Polman, J. Appl. Phys. **75**, 173 (1994).
[6] S.I. Najafi, *Introduction to Glass Integrated Optics*, edited by S. I. Najafi (Artech House, Boston, 1992).
[7] V.A. Ganshin and Yu.N. Korkishko, Opt. Commun. **86**, 523 (1991).
[8] V.Sh. Ivanov, V.A. Ganshin, and Yu.N. Korkishko, Vacuum **43**, 317 (1991).
[9] G.C. Righini, M. Brenci, M.A. Forastiere, S. Pelli, G. Ricci, G.N. Conti, N. Peyghambarian, M. Ferrari, and M. Montagna, Philos. Mag. B **82**, 721 (2002).
[10] R.H. Doremus, J. Phys. Chem. **68**, 2212 (1964).
[11] R. Terai and R. Hayami, J. Non-Cryst. Solids **18**, 217 (1975).
[12] M. Abou-El-Leil and F. Leonberger, J. Am. Ceram. Soc. **71**, 497 (1988).
[13] Y.N. Korkishko and V.A. Fedorov, *Ion Exchange in Single Crystals for Integrated Optics and Optoelectronics* (Cambridge International Science, Cambridge, 1999).
[14] A.N. Milliou, R. Srivastava, and R.V. Ramaswamy, Appl. Opt. **30**, 674 (1991).
[15] C. Sada, E. Borsella, F. Caccavale, F. Gonella, F. Segato, Yu.N. Korkishko, V.A. Fedorov, T.V. Morozova, G. Battaglin, and R. Polloni, Appl. Phys. Lett. **72**, 3431 (1998).
[16] F. Caccavale, C. Sada, F. Segato, Yu.N. Korkishko, V.A. Fedorov, and T.V. Morozova, J. Non-Cryst. Solids **245**, 135 (1999).
[17] F. Caccavale, C. Sada, F. Segato, B. Allieri, L.E. Depero, L. Sangaletti, Yu.N. Korkishko, V.A. Fedorov, and T.V. Morozova, J. Non-Cryst. Solids **280**, 156 (2001).
[18] C. Sada, F. Caccavale, F. Segato, B. Allieri, and L.E. Depero, Opt. Mater. (Amsterdam, Neth.) **19**, 23 (2002).
[19] A.D. MacGillivray, J. Chem. Phys. **48**, 2903 (1968).
[20] D.L. Huber, D.S. Hamilton, and B.B. Barnet, Phys. Rev. B **16**, 4642 (1977).
[21] A.R. Cooper, J. Non-Cryst. Solids **14**, 65 (1974).
[22] R.V. Ramaswamy and R. Srivastava, J. Lightwave Technol. **6**, 6 (1988).
[23] G. De Marchi, P. Mazzoldi, G. Battaglin, A. Valentini, M. Gaudio, A. Losacco, A. Miotello, and R. Dal Maschio, Proc. SPIE **1128**, 117 (1989).
[24] A. Quaranta, Ph.D. thesis, University of Padova, Italy, 1993.
[25] F. Gonella, F. Caccavale, L.D. Bogomolova, F. D'Acapito, and A. Quaranta, J. Appl. Phys. **83**, 1200 (1998).
[26] E. Borsella, G. De Marchi, F. Caccavale, F. Gonella, G. Mattei, P. Mazzoldi, G. Battaglin, A. Quaranta, and A. Miotello, J. Non-Cryst. Solids **253**, 261 (1999).

[27] I. Fainaro, M.I. Shalom, M. Ron, and S. Lipson, J. Phys. Chem. **25**, 16 (1984).
[28] A. Lupascu, A. Kevorkian, T. Boudet, F. Saint-André, D. Persegol, and M. Levy, Opt. Eng. **35**, 1603 (1996).
[29] N. Sarafianos, J. Phys. Chem. **79**, 4 (1975).
[30] R.M. Barrer, R.F. Bartholomew, and L.V.C. Rees, J. Phys. Chem. Solids **24**, 309 (1963).
[31] J.R. Carruthers, I.P. Kaminov, and L.W. Stulz, Appl. Opt. **13**, 2333 (1974).
[32] R.J. Charles, J. Appl. Phys. **32**, 1115 (1961).
[33] D.P. Birnie, J. Mater. Sci. **28**, 302 (1993).
[34] J.R. Crank, *The Mathematics of Diffusion* (Clarendon, Oxford, UK, 1956).
[35] R.R. Hofemann, J. Phys. Chem. **69**, 4226 (1965).
[36] D.A. Okongwu, W.K. Lu, A.E. Hamielec, and J.S. Kirdaldy, J. Chem. Phys. **58**, 777 (1973).
[37] A. Brandenburg, J. Lightwave Technol. **LT4**, 1580 (1986).
[38] A. Rauber, in *Current Topics in Materials Science*, edited by E. Kaldis (North-Holland, Amsterdam, 1978).
[39] R.S. Weis and T.K. Gaylord, Appl. Phys. A: Solids Surf. **37**, 191 (1985).
[40] R.V. Schmidt and I.P. Kaminow, Appl. Phys. Lett. **25**, 458 (1974).
[41] K. Tabata, T. Choso, and Y. Nagasawa, Surf. Sci. **408**, 137 (1998).
[42] Y.S. Kim and R.T. Smith, J. Appl. Phys. **40**, 4637 (1969).
[43] F. Caccavale, A. Morbiato, M. Natali, C. Sada, and F. Segato, J. Appl. Phys. **87**, 1007 (2000).